

52-32
272318
88
N90-21882

The Determination of Maximum Deep Space Station Slew Rates for a High Earth Orbiter

J. A. Estefan
Navigation Systems Section

As developing national and international space ventures, which seek to employ NASA's Deep Space Network (DSN) for tracking and data acquisition, evolve, it is essential for navigation and tracking system analysts to evaluate the operational capability of Deep Space Station antennas. To commission the DSN for use in tracking a highly eccentric Earth orbiter could quite possibly yield the greatest challenges in terms of slewing capability; certainly more so than with a deep-space probe. This article focuses on the determination of the maximum slew rates needed to track a specific high Earth orbiter, namely, the Japanese MUSES-B spacecraft of the Very Long Baseline Interferometry Space Observatory Program. The results suggest that DSN 34-m antennas are capable of meeting the slew rate requirements for the nominal MUSES-B orbital geometries currently being considered.

I. Introduction

The Institute for Space and Astronautical Science (ISAS) has proposed the implementation of an orbiting radio telescope observatory mission known as the Very Long Baseline Interferometry (VLBI) Space Observatory Program (VSOP) for launch in the mid-1990s timeframe. The program is structured to be an international collaboration of the VLBI radio astronomy communities of the United States, Europe, and Australia, as well as other interested nations, with the intention of providing a worldwide observatory network.

ISAS and NASA will undertake a cooperative effort for precise tracking of VSOP's MUSES-B spacecraft by commissioning NASA's Deep Space Network (DSN) together with various Japanese ground stations.

Due to the highly eccentric orbit proposed for MUSES-B, concern arose as to whether or not DSN 34-m antennas would be capable of slewing fast enough to follow the spacecraft. An effort was undertaken to formulate an analytic model for the determination of antenna slew angles (i.e., azimuth and elevation angles), as well as antenna slew rates, and produce a computer program for generating their corresponding time histories. Analysis of different scenarios together with knowledge of the operational slewing capability of the Deep Space Station (DSS) antennas would thereby yield tracking feasibility results.

This article details the modeling and analysis process of this effort as well as results and implications of a few selected mission scenarios. Results indicate that DSN 34-m antennas are indeed capable of meeting slewing

requirements for MUSES-B's nominal mission orbit and, more importantly, further preliminary studies can now be readily performed for future planned missions.

II. Modeling Assumptions and Analysis

In order to arrive at an analytical formulation of the problem, the spacecraft orbit was modeled with two-body dynamics. The Earth's precession of equinoxes was *not* modeled. Classical orbital elements were assumed time-invariant as were the cylindrical coordinates of the station position.¹ The derivation of the azimuth and elevation angles in a (north, east, down) topocentric-horizon reference frame yielded inverse trigonometric functions of the station-to-spacecraft slant range vector. The actual equations are omitted here for brevity. Once the analytical expressions for the slant range vector were derived, analytical expressions for the time-rates-of-change of azimuth and elevation could be determined. It should be noted that expressions for the slant range vector components were derived as functions of the time-varying parameters of station right-ascension, $\theta(t)$, and spacecraft eccentric anomaly, $E(t)$; together with the time-invariant parameters of the classical elements, station position components, and associated direction-cosine terms.

Despite the fact that a simple model was used for this study, the analytical expressions for azimuth and elevation angle determination and their corresponding time-rates-of-change were too lengthy to obtain a time history of results by hand. The expressions were mechanized in a computer program to facilitate rapid evaluation of different cases. Input/Output specifications are listed below.

A. Inputs

The inputs are r_s , λ_{sta} , z_0 , θ_{g0} , ω_\oplus , a , e , Ω , i , ω , μ_\oplus , E_0 , t_0 , dt , t_{STOP} where

- r_s = station distance from Earth's spin axis (km)
- λ_{sta} = station longitude (east of prime meridian) (deg)
- z_0 = station distance above equatorial plane (km)
- θ_{g0} = Greenwich mean sidereal time (sec)
- ω_\oplus = Earth's rotation rate (rad/sec)
- a = semi-major axis (km)
- e = eccentricity
- Ω = longitude of the ascending node (deg)

- i = inclination (deg)
- ω = argument of perigee (deg)
- μ_\oplus = Earth's gravitational parameter (km^3/sec^2)
- E_0 = initial spacecraft eccentric anomaly (sec)
- t_0 = specified epoch time (sec)
- dt = time increments (sec)
- t_{STOP} = program stop time (sec)

B. Outputs

The outputs are t , $\theta = \theta(t)$, $E = E(t)$, $Az = Az(\theta, E, t; p)$, $El = El(\theta, E, t; p)$, $\dot{t} = \dot{\theta}(t)$, $\dot{E} = \dot{E}(t)$, $\dot{Az} = \dot{Az}(\theta, E, t; p)$, $\dot{El} = \dot{El}(\theta, E, t; p)$ (\dot{Az})_{max}, (\dot{El})_{max} where

- t = time (hrs)
- θ = station right-ascension (deg)
- E = spacecraft eccentric anomaly (deg)
- Az = azimuth angle (deg)
- El = elevation angle (deg)
- \dot{Az} = azimuth rate (deg/sec)
- \dot{El} = elevation rate (deg/sec)
- p = input parameter set

III. Results and Implications

A case-by-case synopsis is provided for three relevant mission scenarios. Tables of input parameters are included as are plotted slew angle time histories. The referenced epoch was taken to be January 1, 1995 at 0^{hr}0^{min}0^{sec} and duration of each run was seventy-two hours. The orbit period in all cases was approximately 6.06 hours.

A. Case 1: (MUSES-B Nominal Orbit; DSS 10)²

The Deep Space Station represented in this case is located at Goldstone, California. Input parameters are listed in Table 1 while plotted results of slew angles are illustrated in Figs. 1 and 2.

Maximum slew rates for this case were found to be approximately

- 0.14 deg/s in azimuth
- 0.10 deg/s in elevation

B. Case 2: (MUSES-B Nominal Orbit; DSS 40)

This scenario was identical to Case 1 with the exception that the Deep Space Station represented is located at

¹ T. Moyer, "Station Location Sets Referred to the Radio Frame," JPL IOM 314.5-1334 (internal document), Jet Propulsion Laboratory, Pasadena, California, February 24, 1989.

² A. Konopliv, "Preliminary Orbit Determination Analysis for the VSOP Mission," JPL IOM 314.5-648 (internal document), Jet Propulsion Laboratory, Pasadena, California, February 9, 1989.

Canberra, Australia. The input parameters are listed in Table 2. Plotted results of slew angles are illustrated in Figs. 3 and 4.

Maximum slew rates for this case were found to be approximately

0.14 deg/s in azimuth

0.09 deg/s in elevation

C. Case 3: (MUSES-B Nominal Orbit; DSS 60)

This scenario was also identical to Case 1 with the exception that the Deep Space Station represented is located at Madrid, Spain. The input parameters are listed in Table 3. Plotted results of slew angles are illustrated in Figs. 5 and 6.

Maximum slew rates for this case were found to be approximately

0.14 deg/s in azimuth

0.08 deg/s in elevation

IV. Conclusions

Maximum slew rates for a DSN 34-m antenna are roughly 0.40 deg/s in both azimuth and elevation *and*, hence, the 34-m antenna would certainly be capable of meeting slewing requirements for any of the case scenarios described above.

Station view periods can also be determined by examining elevation angle time histories that are generated by the computer program. Fig. 7 provides an example of this capability, which represents Cases 1 through 3 employing an elevation cutoff angle of ten degrees above the local horizon.

Acknowledgment

The author would like to express a note of appreciation for those who assisted in this work effort. In particular, a warm thanks to Alex Konopliv for providing initial guidance to problem modeling. A very special thanks to Sam Thurman for providing invaluable guidance and assistance in all aspects of the study.

Table 1. Input parameter set for Case 1

$\frac{r_s(\text{km})}{5204.00}$	$\frac{\lambda_{sta}(\text{deg})}{243.1105}$	$\frac{z_0(\text{km})}{3677.05}$
$\frac{\theta_{g0}(\text{deg})}{100.175}$	$\frac{\omega_{\oplus}(\text{rad/sec})}{7.292116 \times 10^{-5}}$	
$\frac{a(\text{km})}{16878.00}$	$\frac{e}{0.5629}$	$\frac{\Omega(\text{deg})}{0.00}$
$\frac{i(\text{deg})}{46.00}$	$\frac{\omega(\text{deg})}{0.00}$	
$\frac{\mu_{\oplus}(\text{km}^3/\text{sec}^2)}{3.9860045 \times 10^5}$	$\frac{E_0(\text{deg})}{0.00}$	
$\frac{t_0(\text{sec})}{0.00}$	$\frac{dt(\text{sec})}{1200.00}$	$\frac{t_{STOP}(\text{sec})}{2.592 \times 10^5}$

Table 3. Input parameter set for Case 3

$\frac{r_s(\text{km})}{4862.45}$	$\frac{\lambda_{sta}(\text{deg})}{355.752}$	$\frac{z_0(\text{km})}{4115.11}$
$\frac{\theta_{g0}(\text{deg})}{100.175}$	$\frac{\omega_{\oplus}(\text{rad/sec})}{7.292116 \times 10^{-5}}$	
$\frac{a(\text{km})}{16878.00}$	$\frac{e}{0.5629}$	$\frac{\Omega(\text{deg})}{0.00}$
$\frac{i(\text{deg})}{46.00}$	$\frac{\omega(\text{deg})}{0.00}$	
$\frac{\mu_{\oplus}(\text{km}^3/\text{sec}^2)}{3.9860045 \times 10^5}$	$\frac{E_0(\text{deg})}{0.00}$	
$\frac{t_0(\text{sec})}{0.00}$	$\frac{dt(\text{sec})}{1200.00}$	$\frac{t_{STOP}(\text{sec})}{2.592 \times 10^5}$

Table 2. Input parameter set for Case 2

$\frac{r_s(\text{km})}{5205.25}$	$\frac{\lambda_{sta}(\text{deg})}{148.9813}$	$\frac{z_0(\text{km})}{-3674.75}$
$\frac{\theta_{g0}(\text{deg})}{100.175}$	$\frac{\omega_{\oplus}(\text{rad/sec})}{7.292116 \times 10^{-5}}$	
$\frac{a(\text{km})}{16878.00}$	$\frac{e}{0.5629}$	$\frac{\Omega(\text{deg})}{0.00}$
$\frac{i(\text{deg})}{46.00}$	$\frac{\omega(\text{deg})}{0.00}$	
$\frac{\mu_{\oplus}(\text{km}^3/\text{sec}^2)}{3.9860045 \times 10^5}$	$\frac{E_0(\text{deg})}{0.00}$	
$\frac{t_0(\text{sec})}{0.00}$	$\frac{dt(\text{sec})}{1200.00}$	$\frac{t_{STOP}(\text{sec})}{2.592 \times 10^5}$

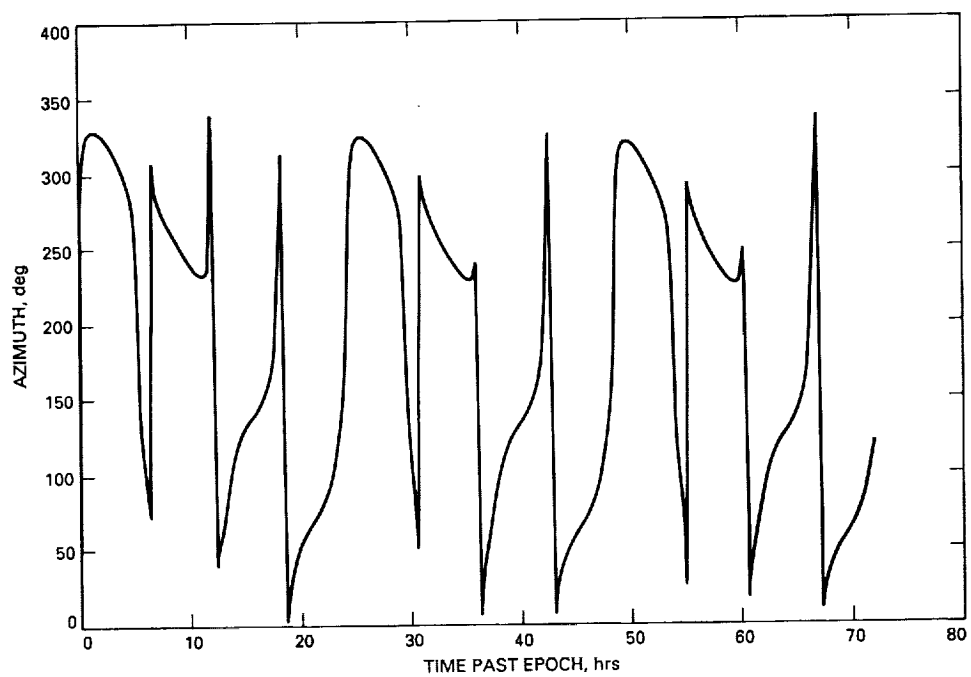


Fig. 1. Azimuth versus time (Case 1).

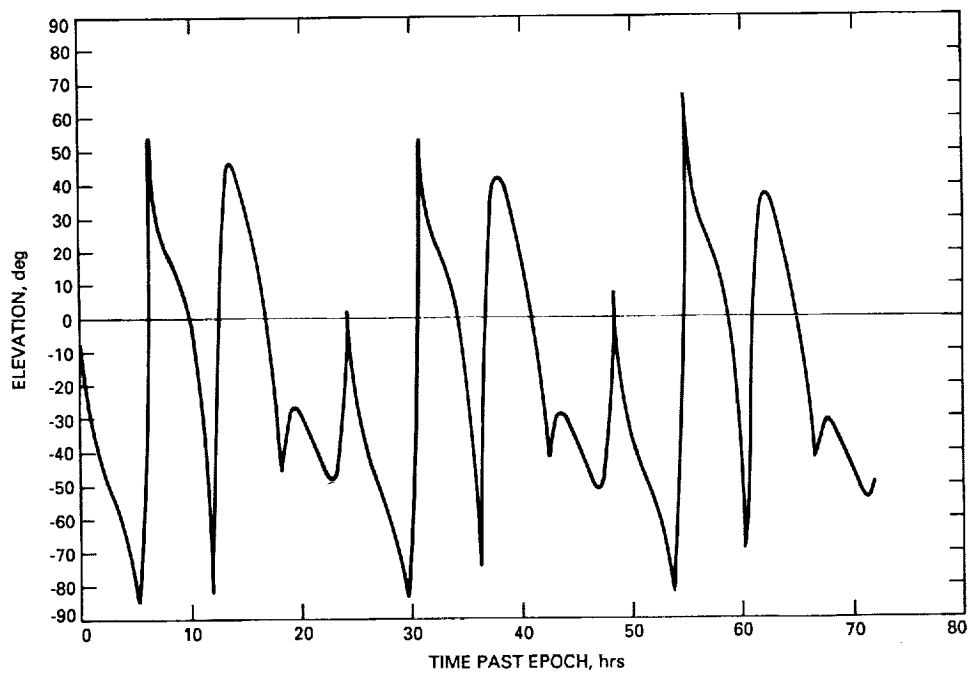


Fig. 2. Elevation versus time (Case 1).

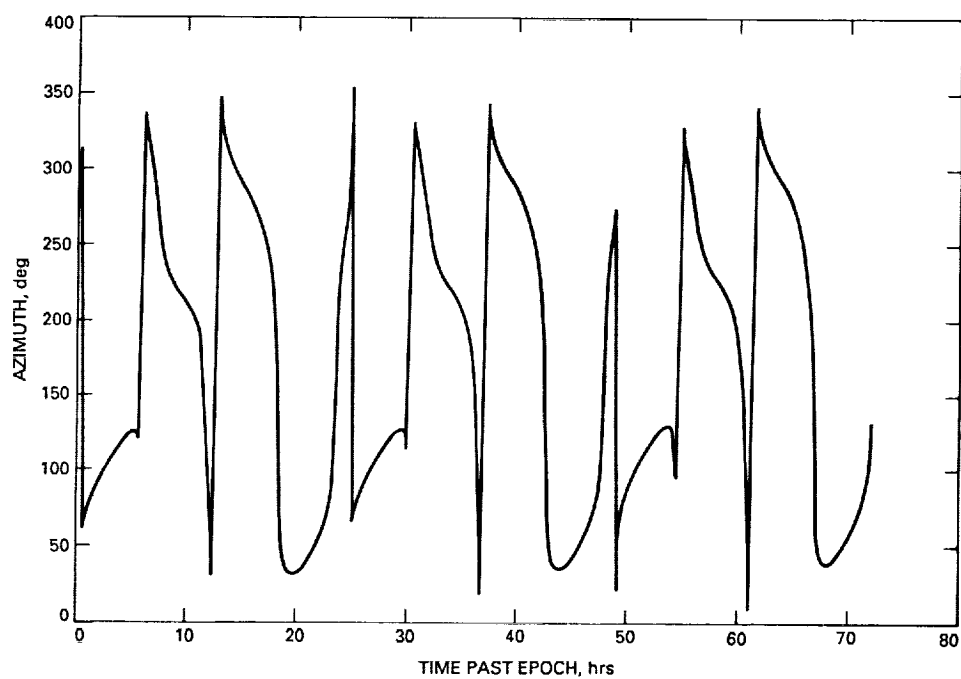


Fig. 3. Azimuth versus time (Case 2).

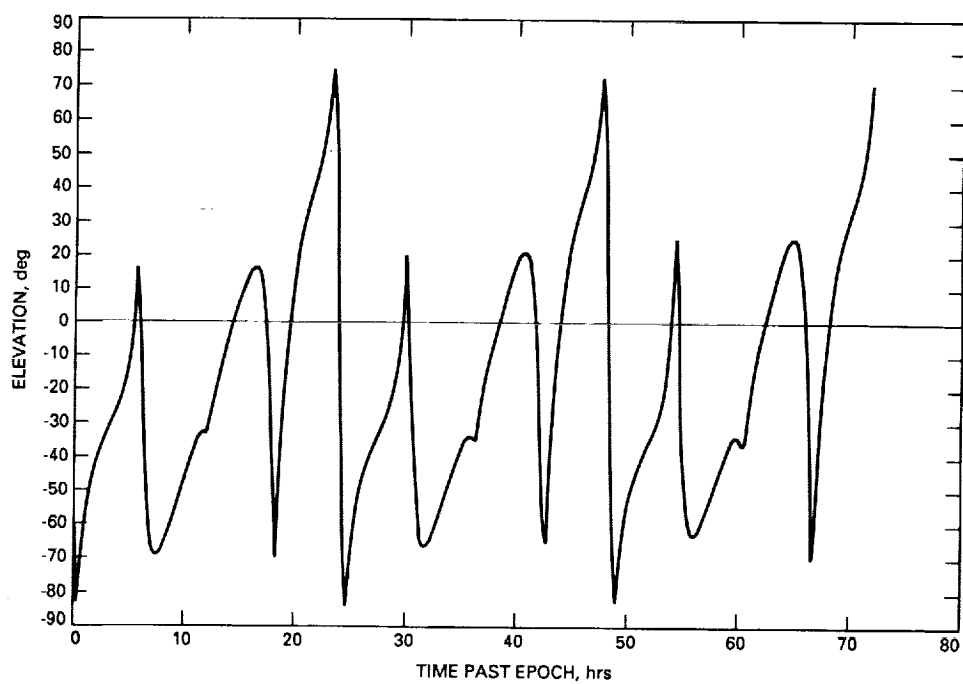


Fig. 4. Elevation versus time (Case 2).

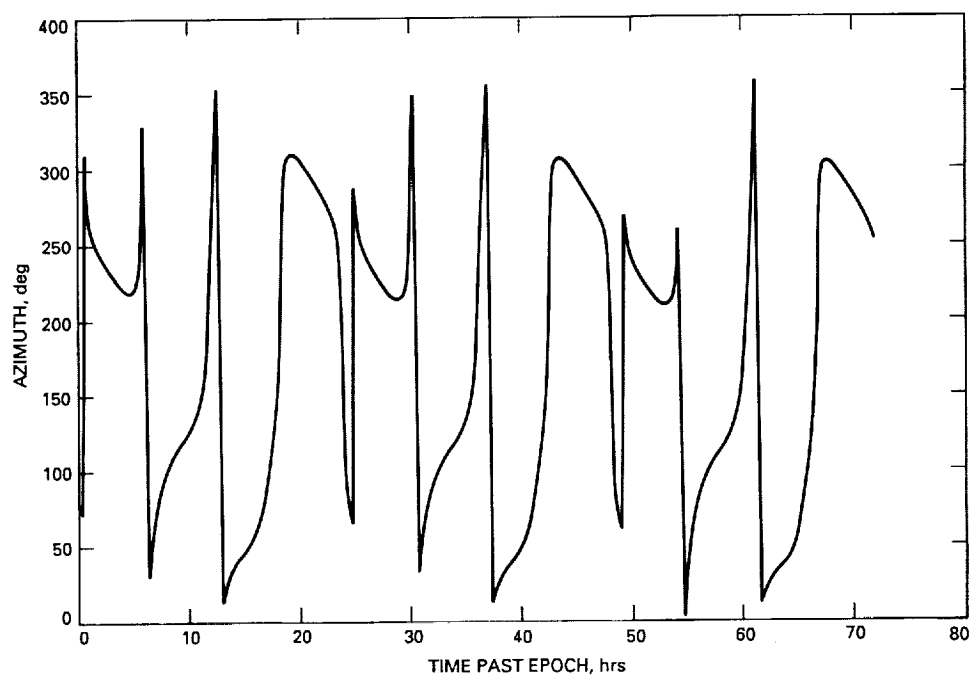


Fig. 5. Azimuth versus time (Case 3).

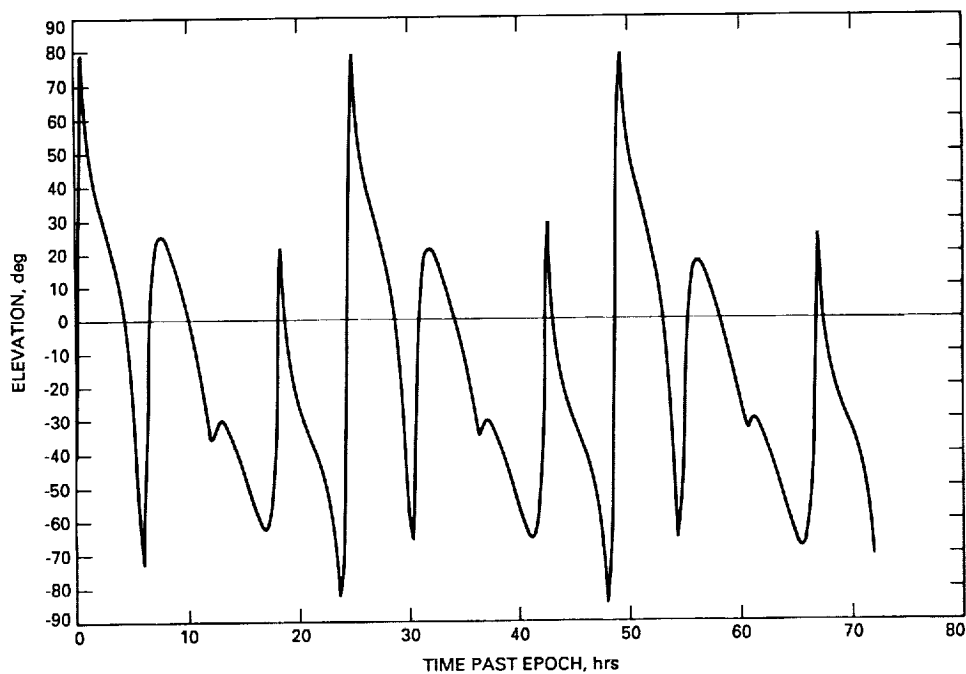


Fig. 6. Elevation versus time (Case 3).

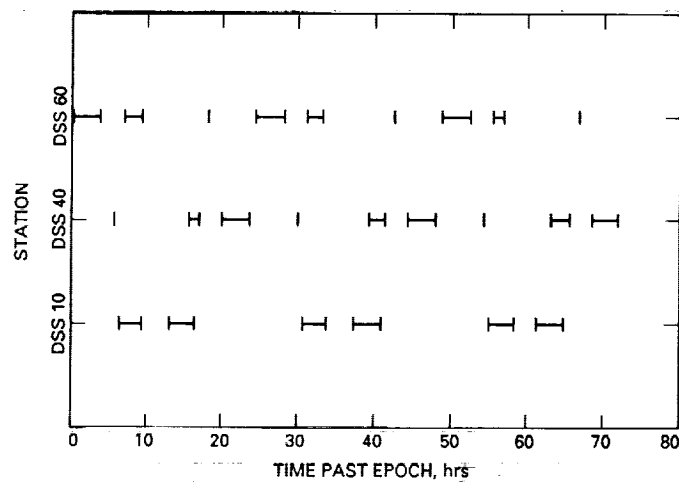


Fig. 7. DSS view periods with 10-deg lower elevation cutoff, epoch 1995-01-01 00:00:00.0000.